

13.2 A fracture mechanics based description of the pull-out behavior of headed studs embedded in concrete (Contribution by R. Eligehausen and G. Sawade)

13.2.1 Introduction

Headed studs embedded in a large concrete block subjected to tension loading fail - provided the steel strength of the stud is high enough - by pulling a cone out of the concrete. The circumferential crack forming this cone is generated and growing in a so-called mixed mode.

Several attempts have been made to understand this crack growth and to predict the pull-out load of headed studs.

Stone/Carino /1/ and Krenchel/Shah /2/ tested headed anchors embedded in concrete. The test set-up was similar to the so-called LOK-test. In both investigations a stable growth of the circumferential crack was found.

Ballarini et.al. /3/ describe the crack propagation in the concrete (using a two-dimensional model) by applying the criterion of a K_{IC} -value at the tip of the crack. According to their investigations the crack growth is stable if the specimen is supported close to the anchor as in the LOK-test. This agrees with /1,2/. If the studs are anchored in a half space with a support far away from the point of loading crack propagation is unstable.

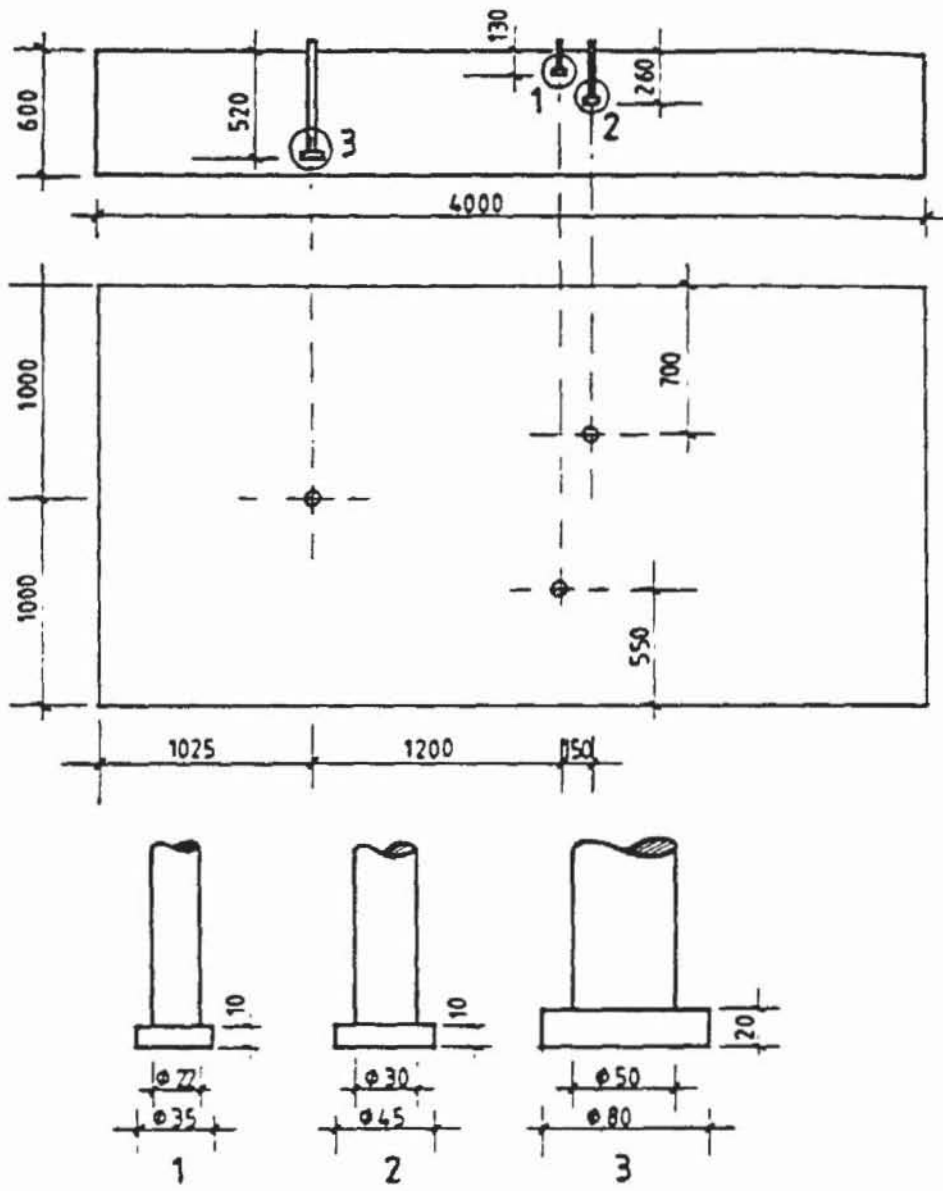
On the contrary to /3/, in the experimental investigations with headed studs anchored in concrete /4/ stable propagation of the circumferential crack was found even in the case of a support relatively far away from the anchor. This result might be due to the fact that the bearing area of the head was relatively small so that approximately a "point" - load was applied. Furthermore the test results might have been influenced by the fact that the test specimen was not axial symmetric.

Therefore more pull-out tests with headed studs embedded in large concrete blocks were performed. Strains in the concrete in the anticipated area of the failure cone were measured using special strain gages. The test results were compared with analytical predictions of crack propagation and failure load.

13.2.2 Experimental Investigations

Pull-out tests were performed with headed studs embedded in large concrete blocks and loaded in tension. The embedment depth was $h_v = 130 - 520$ mm (Fig. 1). The test specimen was a concrete slab with the dimensions length/width/ thickness = 4/2/0,6 m with structural surface reinforcement. This reinforcement had no significant influence on the test results. Composition and characteristics of the concrete are given in table 1.

In the tests, the displacement of the headed studs was continuously increased. The reaction forces were introduced onto the concrete at a distance $\geq 1,75 h_v$ from the stud (Fig. 2).



dimensions in mm

Fig. 1: Dimensions of test specimen and headed studs

Cement PZ 35 F : 200 kg/m³
 Water : 188 kg/m³
 Aggregates 0 - 16 mm: 1893 kg/m³
 Grading curve between lines A 16 and B 16 after DIN 1045

a) Composition

Compression strength (cylinders

with h = 150 mm, d = 150 mm)

$$f_c = 22,9 \text{ N/mm}^2$$

Axial tension strength

$$f_t = 1,8 \text{ N/mm}^2$$

Modulus of elasticity

$$E_c = 23500 \text{ N/mm}^2$$

Total crack formation energy

$$G_F = 0,07 \text{ N/mm}$$

b) Properties

Table 1: Composition and properties of the concrete

Embedment depth	Maximum load	Load at crack initiation	
		Detection by	
		Sound emission analysis	Strain measure- ments
mm	kN	kN	kN
130	97,2	not measured	19
260	290,2	100	58
520	885,2	175	159

Table 2: Test results

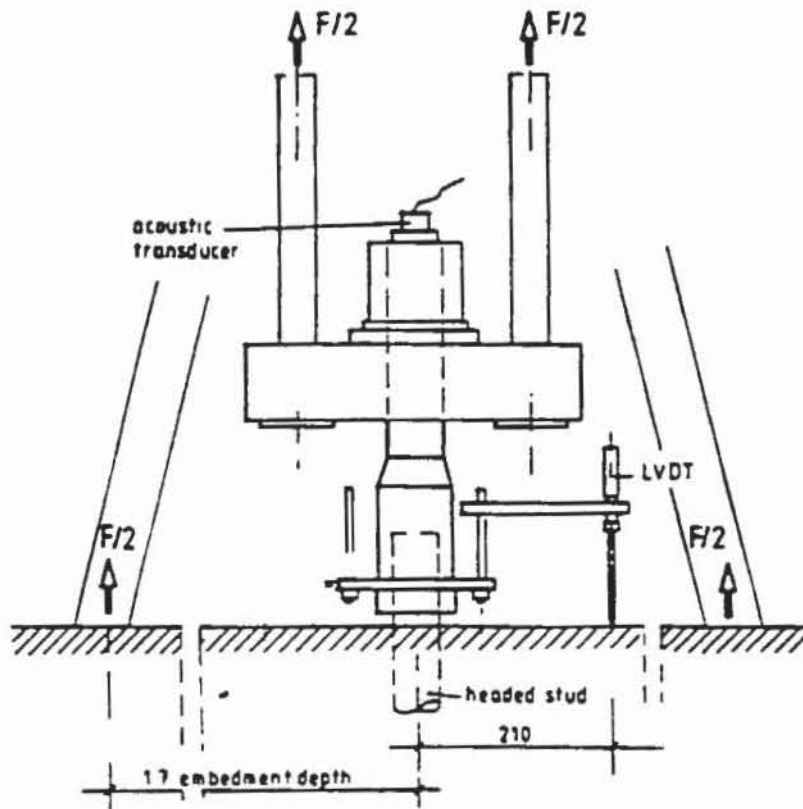
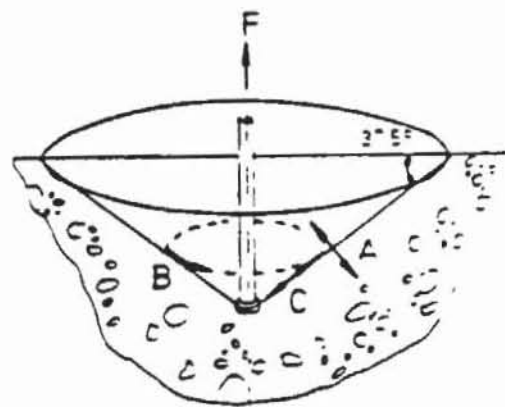


Fig. 2: Test set-up



Strain measurement
 A) perpendicular,
 B) circumferential,
 C) parallel to the crack surface

Fig. 3: Strain measurements
 in the concrete

The cracking- and deformation behavior in the interior of the concrete in the region of the expected failure cone was measured by special strain gages (Type PML of Tokyo Sokki Comp.). They were installed perpendicularly (A), circumferentially (B) and parallel (C) to the failure cone surface (Fig. 3). Length and position of the strain gages were chosen so that they crossed or were parallel to the expected crack in the interior of the concrete. The form of the failure cone was known by preliminary tests. The inclination between failure cone generatrice and concrete surface was $37,5^\circ$ on the average. Moreover sound emission analysis was used to detect crack initiation and formation.

Main test results are given in table 2. In Fig. 4 the observed load displacement relationships are plotted. Fig. 5 shows the strains measured along the surface of the later failure cone in direction A (perpendicular to the expected crack direction) for two load levels ($F/F_{\max} = 0,3; 0,9$). The figure is valid for an embedment depth $h_v = 520$ mm.

It can clearly be seen that with increasing loads the area of great strain gradients is moving from the loaded region towards the concrete surface. This is an indication for a change in the bearing behavior due to crack formation.

The stresses perpendicular to the crack surface were calculated from the measured strains. It was assumed that the measured strains ϵ_A in direction A (cf. Fig. 3) are given by addition of the elastic strain ϵ_{el} of the concrete and the strain due to crack opening w perpendicular to the crack surface related to the length l_M of the strain gages:

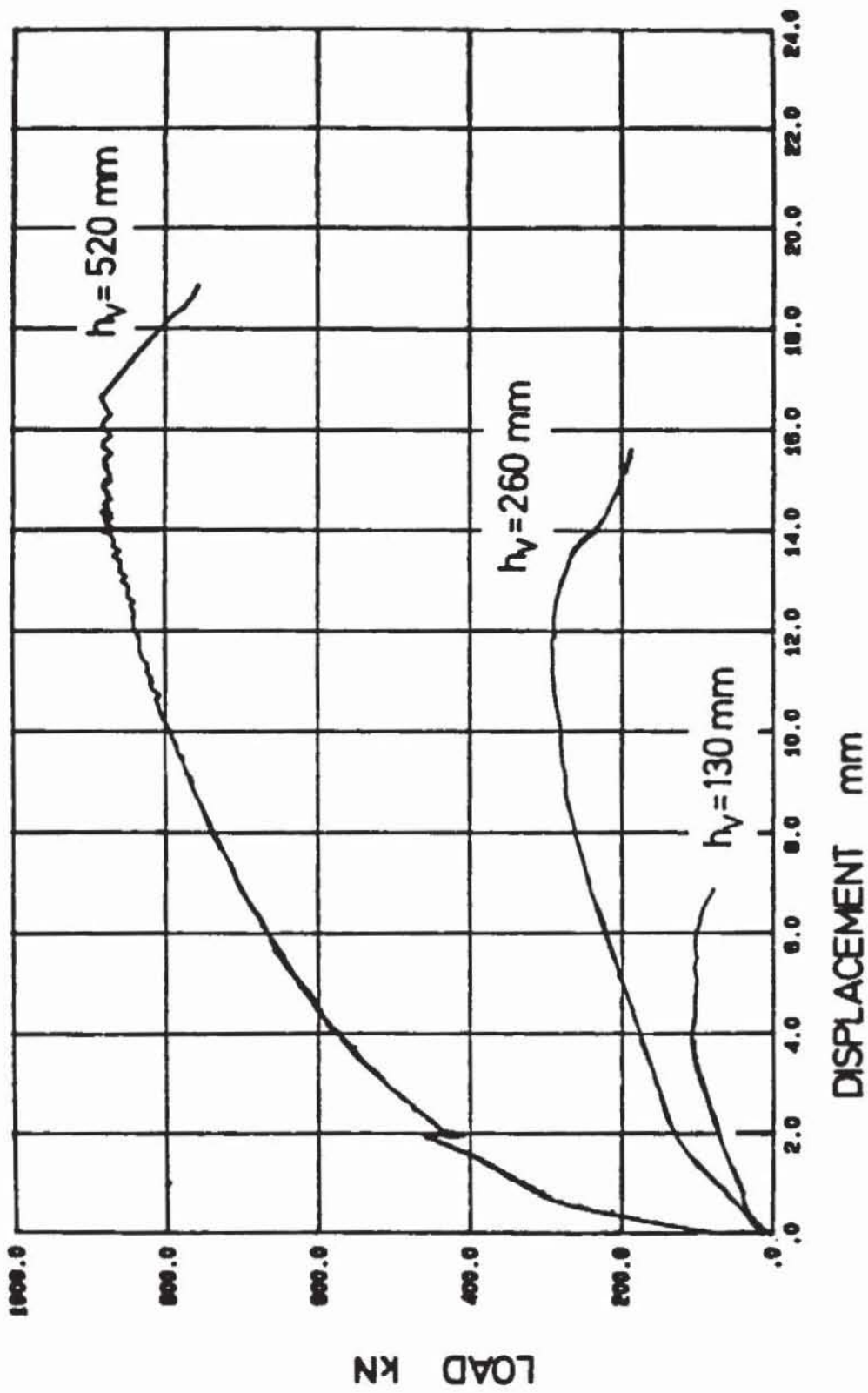


Fig. 4: Load as a function of the observed displacement of the anchor relative to the concrete surface

$$\epsilon_A = \epsilon_{el} + \frac{w}{l_M} = \frac{\sigma(w)}{E_C} + \frac{w}{l_M} \quad (1)$$

E_C - modulus of elasticity of the concrete

l_M - measuring length of strain gage

According to /4,5/ the transfer of normal stresses across the crack can be expressed by

$$\sigma(w) = B_Z \cdot \exp(-(f_t/G_F) \cdot w) \quad (2)$$

f_t - axial tensile strength

G_F - total crack formation energy

w - crack width

From equations (1) and (2) results a non-linear relation for the normal stress $\sigma(w)$ which can be solved iteratively.

Fig. 6 shows the calculated distribution of tensile stresses along the failure cone surface. The effect of stress redistribution due to stable crack growth can clearly be seen by the shifting of the place of maximum tensile stress towards the concrete surface for increasing loads. Stable crack growth was also confirmed by sound emission analysis.

In Fig. 7 the ratio cracked surface to total surface of the failure cone is plotted as a function of the load on the anchor. The transition point between the cracked zone (cracking process zone) and the uncracked concrete has been assumed where the critical strain

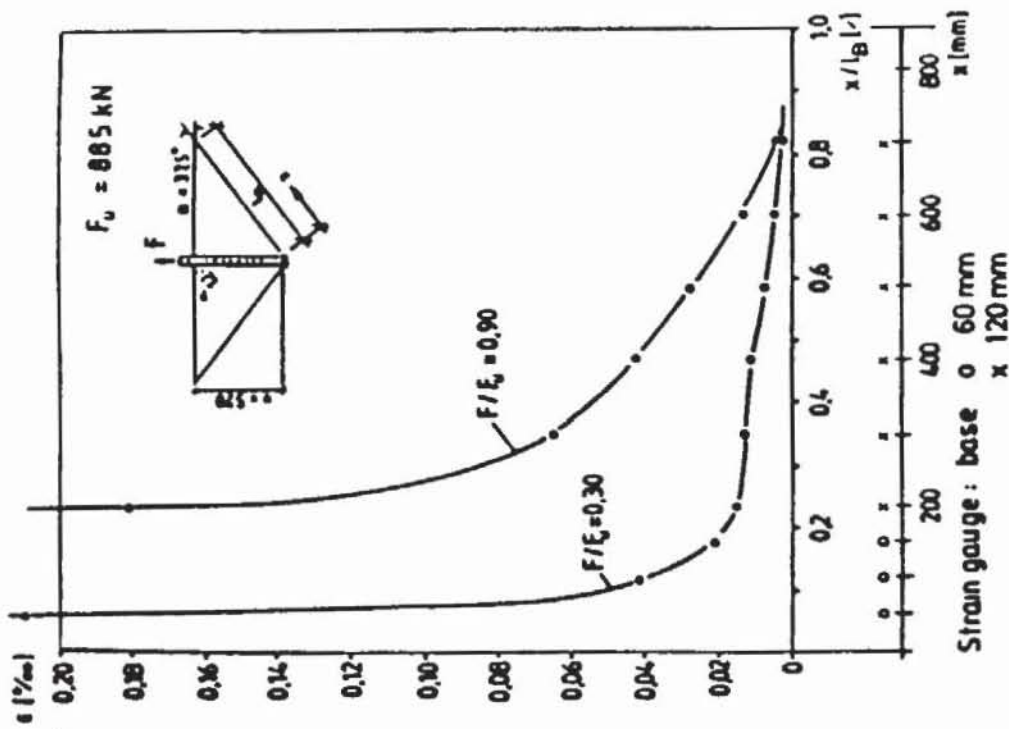


Fig. 5: Distribution of strains perpendicular to the failure cone surface

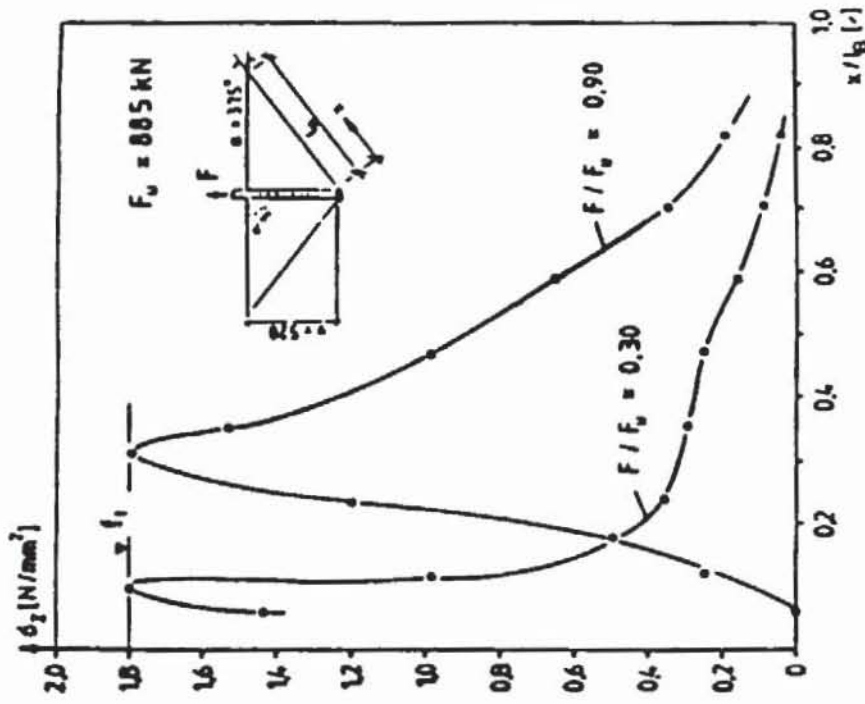


Fig. 6: Distribution of tensile stresses perpendicular to the failure cone surface

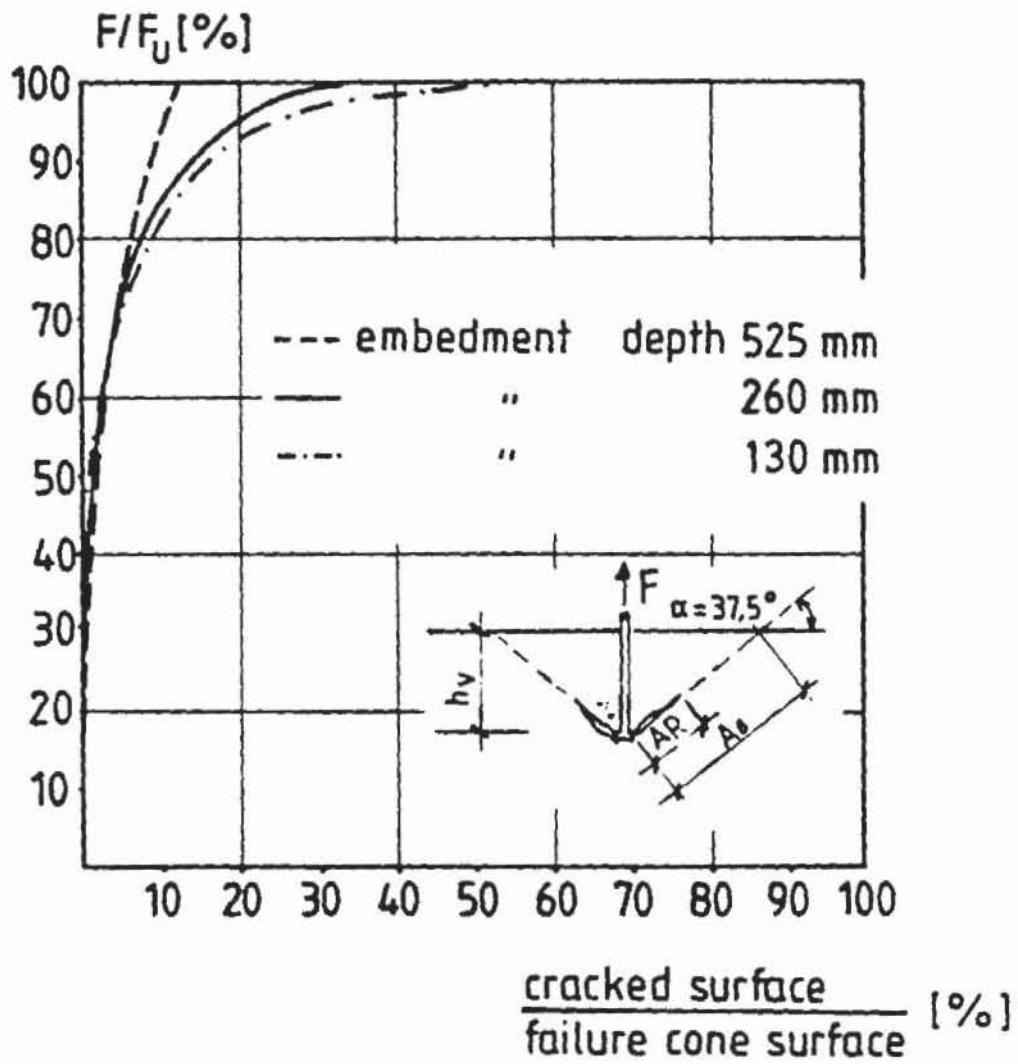


Fig. 7: Ratio cracked surface to total surface of failure cone

$\epsilon \approx 0,08$ o/o and thus the tensile strength has been reached. Due to the cone-shaped crack the ratio cracked surface/total cone surface is rather low even at maximum load - especially for headed studs with a large embedment depth $h_v = 520$ mm.

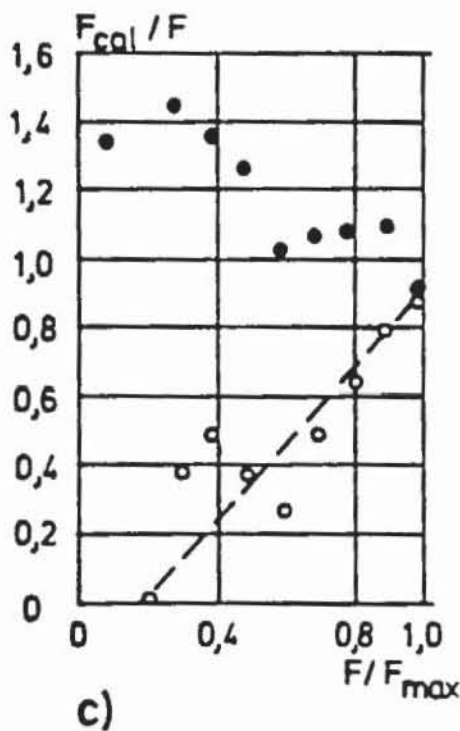
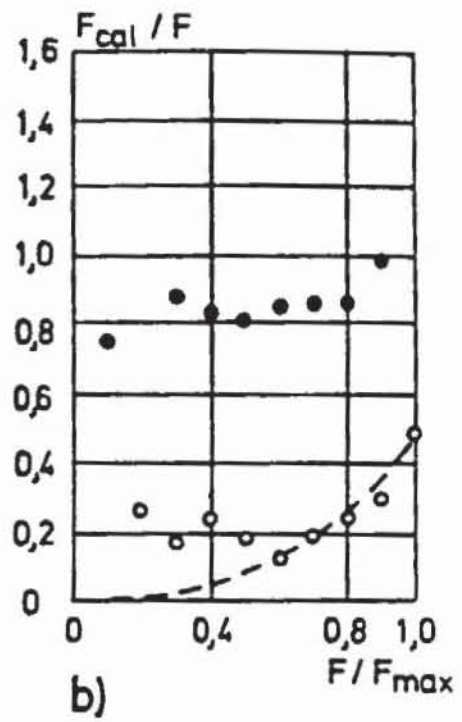
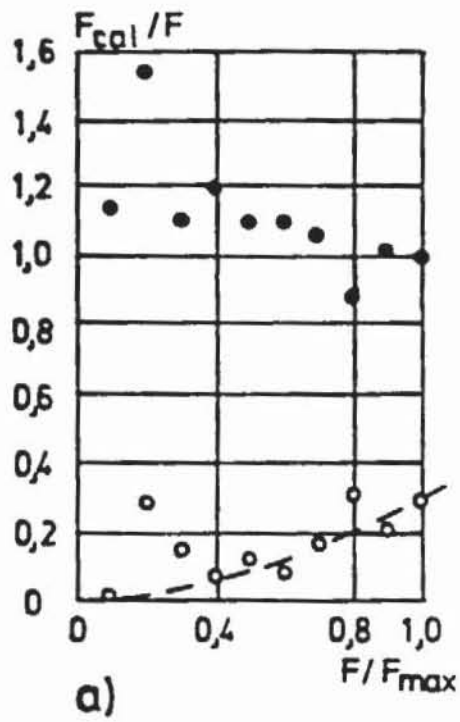
The component in direction of the applied tensile load of the normal stresses perpendicular to the failure cone (cf. Fig. 6) has been integrated over the total cone surface and the cracked surface respectively.

Fig. 8 shows the calculated tensile forces related to the applied load as function of the loading. For loadings higher than 50 % of the measured maximum load the calculated total tensile forces differ from the measured ones up to a maximum of 15 %. It can be concluded, therefore, that in the investigated case shear stresses on the crack surface have only a negligible influence on the load transfer and that the surface energy required for crack formation in a so-called mixed-mode may be estimated by the material parameter G_F .

The ratio force transferred in the crack process zone to total load is decreasing with increasing embedment depth. This means that the bearing behavior of fastenings with great embedment depths can be approximated by linear fracture mechanics.

13.2.3 Theoretical Investigations

For the description of failure processes an energetic model has been developed taking into account the energy and entropy balance of the specimen /6/. The material



● $F(\text{calculation}) / F(\text{test})$
 ○---○ $F_r(\text{calculation}) / F(\text{test})$
 $F_r =$ load transferred in the micro crack zone

Fig	V (mm)	F_{max} (KN)
a)	520	885
b)	260	290
c)	130	97

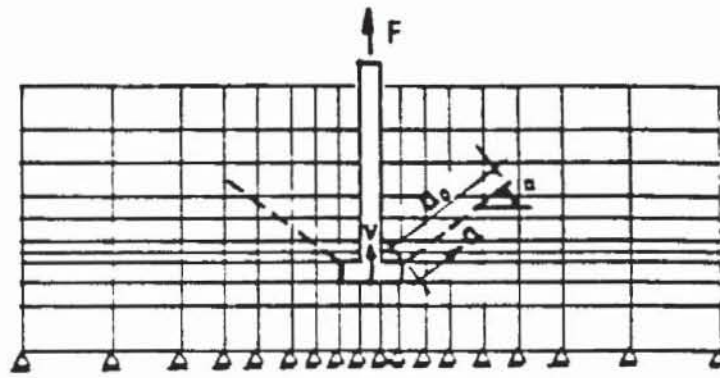
Fig. 8: Ratio calculated tensile load to applied load as a function of the loading

behavior is described by relations for the free energy and entropy production as a function of mechanical variables and their changes with time. The displacement field, the crack contour, the crack openings and the plastic strains are regarded as mechanical variables. For monotonic loading the crack formation is defined by the condition that the free energy (sum of elastic deformation energy and surface energy) becomes a minimum.

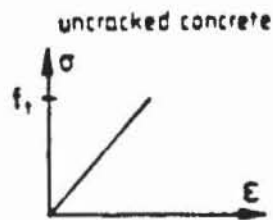
Fig. 9 shows the application of this fracture mechanics model on a headed stud embedded in concrete. For simplification only the formation of an axially symmetrical, circumferential discrete crack is considered (Fig. 9a). The concrete in immediate vicinity of the crack is modelled as linear-elastic material (Fig. 9b). In a non linear fracture mechanics approach the crack formation is represented by the specific crack formation energy $G(w)$ (Fig. 9c) which is the required energy per unit crack surface for the generation of a crack with the opening w . From the function $G(w)$ the axial tensile strength f_t and the total specific crack surface energy G_F can be derived (cf. Hillerborg /7/). From the variation of the total free energy with the crack length and the crack angle respectively the length of the crack and its contour may be obtained as function of the induced load (Fig. 9d).

Due to reasons given in chapter 2 (cf. Fig. 7 and 8) for the special case of a large embedment depth the specific crack formation energy may be given using the linear fracture mechanics approach

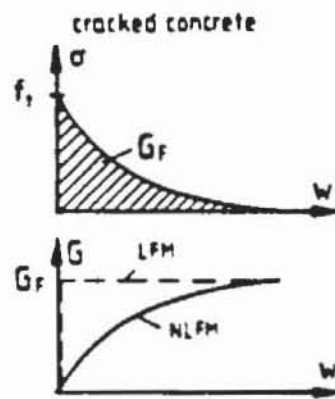
$$G(w) = G_F, w > 0 \quad (3)$$



a)



b)



c)

$$\begin{aligned} \Psi_{TOTAL} &= \Psi_{el} + \Psi_{CRACK SURFACE} = \text{Minimum} \\ &= \frac{1}{2} K(a_0, a) v_0^2 + \int_0^{a_0} G(w(a)) dA(a) \\ K &= \text{System stiffness} \end{aligned}$$

$$\frac{\delta \Psi_{TOTAL}}{\delta a} = 0 \quad \text{; crack length}$$

$$\frac{\delta \Psi_{TOTAL}}{\delta \alpha} = 0 \quad \text{; crack angle}$$

d)

Fig. 9: Application of the theoretical model on headed studs embedded in concrete

The relation between the induced force F and the crack length a is then given by

$$F = (E \cdot G_F)^{1/2} \cdot h_v^{3/2} f(a/l_B) \quad (4)$$

l_B - length of failure cone surface (see fig. 10)

The function $f(a/l_B)$ depends on the crack length achieved on the crack contour. It is given in Fig. 10, which is valid for a "point"-load and a circumferential crack inclined $37,5^\circ$ to the concrete surface as observed in the experiments. It can be seen from Fig. 10 that up to maximum load the crack growth is stable. For a relative crack length $a/l_B \approx 0,45$ the maximum load

$$F_{\max} = 2,1 \cdot (E_C \cdot G_F)^{1/2} \cdot h_v^{3/2} \quad (5)$$

is reached.

Fig. 11 shows the failure loads of headed studs embedded in concrete, calculated by equation (5), as a function of the embedment depth. For comparison the maximum loads measured in the tests and the values calculated by the empirical equation /8/ are given also. The agreement between theory and test results is sufficient for practical purposes.

13.2.4 Summary

According to the experiments the behavior of headed studs embedded in a large concrete block and loaded in tension with the support reactions relatively far away from the anchor is controlled by stable growth of the circumferential failure crack up to maximum load. Just before reaching maximum load the area of cracked con-

$$f(a/l_B) = \frac{F}{\sqrt{EG}} v^{3/2}$$

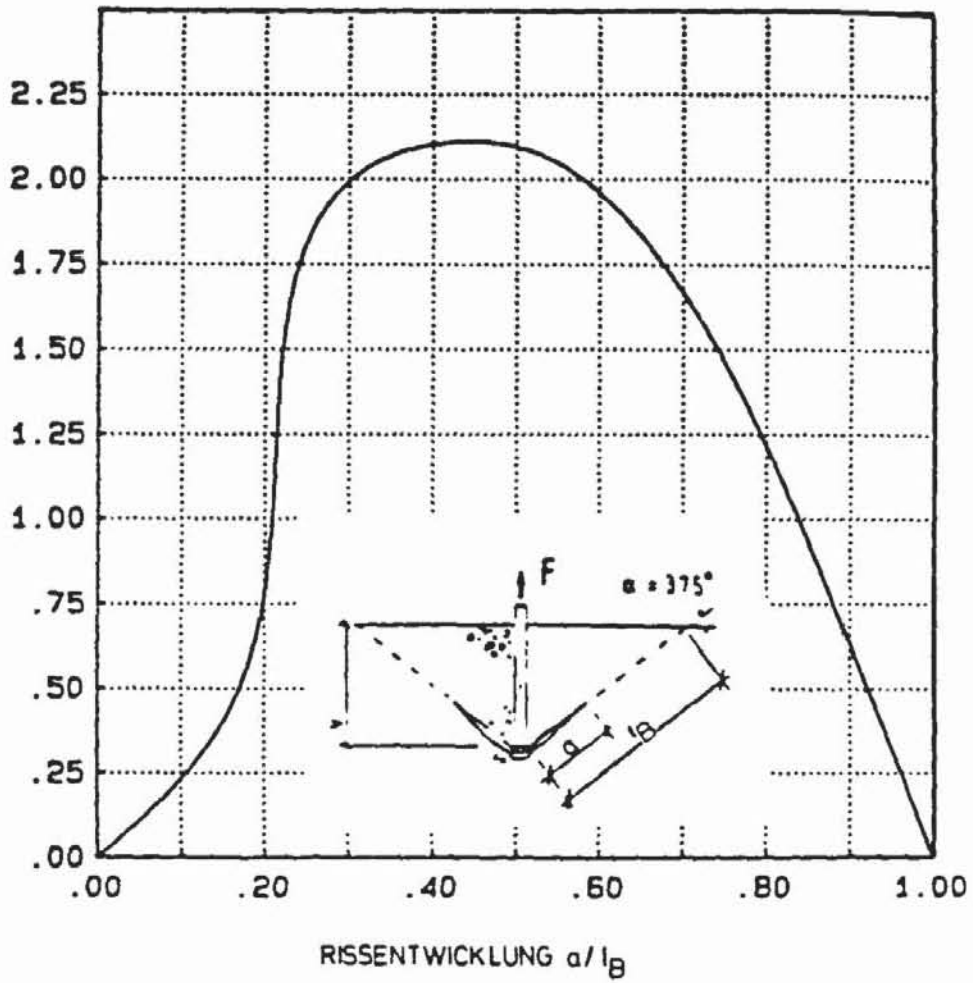


Fig. 10: Calculated load as a function of the crack length a

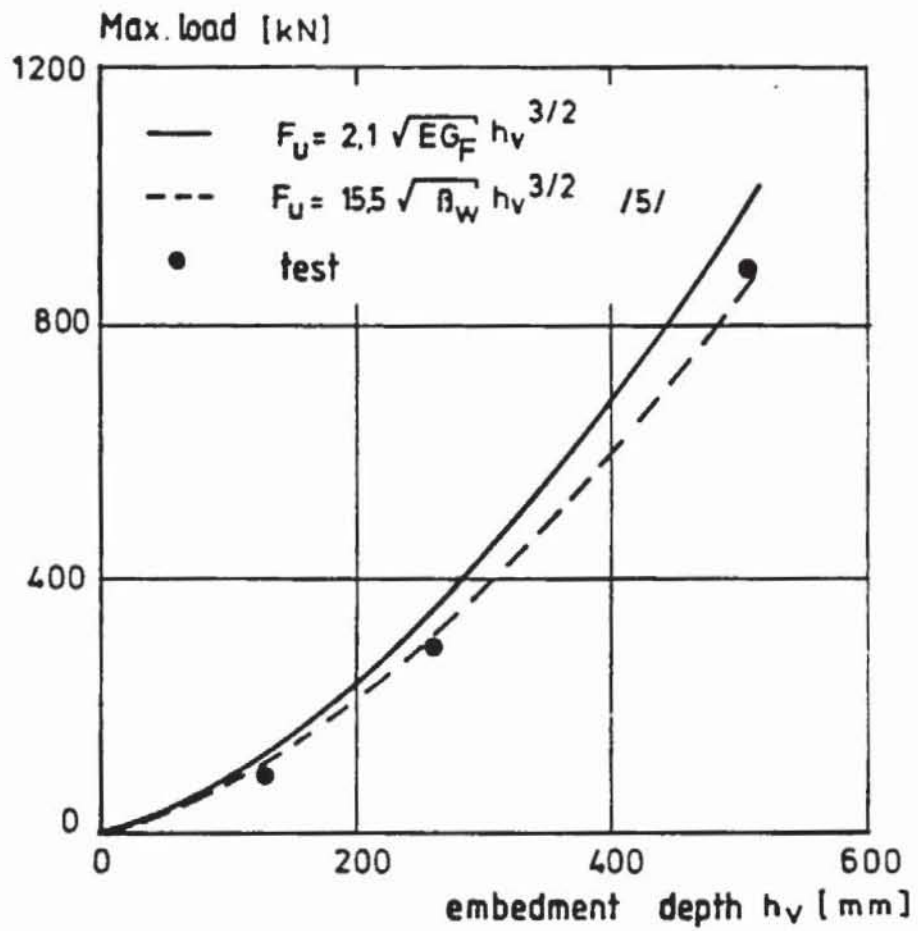


Fig. 11: Concrete cone failure load of headed studs as a function of embedment depth

crete is only some 25 % to 30 % of the whole surface of the fracture cone, which is mainly formed in the descending part of the load-displacement curve. For a large embedment depth ($h_v \geq 260$ mm) the load transferred in the cracked area is relatively small compared to the total load.

The behavior of concrete loaded in tension has been modelled by an energetic approach. In this model crack formation processes during monotonic loading are described by the condition that the free energy (sum of elastic deformation energy and surface energy) becomes a minimum. The specific surface energy G required for crack propagation depends on the crack width. From the function $G(w)$ the concrete tensile strength (for $w = 0$) and the G_F -value may be derived. Concrete outside of discrete cracks is assumed as a linear elastic material.

Using the analytical model with the simplification $G(w) = G_F = \text{const.}$ the observed crack formation and maximum loads of headed studs embedded in concrete could be predicted with sufficient accuracy for practical applications. According to the theoretical investigations the failure load of headed studs anchored in concrete depends on the material parameters E_c and G_F and not - as usually assumed - on the tensile strength. The failure load increases proportionally to $h_v^{3/2}$ which corresponds to the experience made so far /8/.

References

- /1/ Stone, W.C.; Carino, N.J.:
Deformation and Failure in Large-Scale Pull-Out Tests, ACI Journal Nov.-Dez. 1983, P. 501 - 513
- /2/ Krenchel, H.; Shah, S.:
Fracture Analysis of the Pull-Out Test, Material Structures, Volume 108
- /3/ Ballarini, R.; Shah, S.; Keer, L.:
Failure characteristics of short anchor bolts embedded in a brittle material, Proc. R. Soc. London A 404-35-54, 1986
- /4/ Eligehausen, R.; Sawade, G.:
Verhalten von Beton auf Zug (Behavior of concrete in tension). Betonwerk + Fertigteil-Technik, No. 5 und 6, 1985, in German and English
- /5/ Sawade, G.; Eligehausen, R.:
Ein Modell des Betonzugverhaltens (A model for concrete in tension). Report of the Institut für Werkstoffe im Bauwesen, Universität Stuttgart, 1986, in German, not published
- /6/ Sawade, G.:
Beitrag zum Verhalten von zugbeanspruchtem Beton (A contribution to the behavior of concrete in tension). Thesis in preparation
- /7/ Hillerborg, A.:
Analysis of One Single Crack. In: Developments in Civil Engineering, Volume 7: Fracture Mechanics of Concrete, Elsevier, 1983
- /8/ Eligehausen, R.; Fuchs, W.; Mayer, B.:
Tragverhalten von Dübelbefestigungen bei Zugbeanspruchung (Behavior of fastenings under tension loading). Betonwerk + Fertigteil-Technik, No. 12, P. 826 - 832, 1987; No. 1, P. 29 - 35, 1988, in German and English